UNIVERSITY OF BUCHAREST
FACULTY OF CHEMISTRY
DOCTORAL SCHOOL IN CHEMISTRY

DOCTORAL THESIS SUMMARY

The physico-chemical characterization of binary mixtures of active principles and carboxylic acids

PhD student: Cristina Macașoi

PhD supervisor: Prof. dr. Viorica Meltzer

PhD Commission:

President: Prof. dr. Camelia Bala

PhD leader: Prof. dr. Viorica Meltzer

Official reviewers:

1. Prof. dr. Lăcrămioara Popa, Carol Davila University of Medicine and Pharmacy, Bucharest

2. Prof. dr. Mihaela Violeta Ghica, Carol Davila University of Medicine and Pharmacy, Bucharest

3. Conf. dr. Marin Micuț, University of Bucharest, Faculty of Chemistry

2023

Summary

The numbering of figures, tables and bibliographic references is the one in the thesis.

Part II: Original contributions

The original data part is comprised of 5 chapters, following the physico-chemical study of some binary mixtures consisting of active principles (bromazepam, nitrazepam, medazepam and meloxicam) and cyclodextrins/citric acid/tartaric acid.

The first three active ingredients belong to the class of diazepines, which are used in the treatment of insomnia, anxiety and have muscle relaxant, amnesic, antiepileptic and sedative properties. Most of them are hardly soluble in water, so that in order to be quickly absorbed in the body and to obtain a good therapeutic response, their solubility in water must be increased. The aim in the studies undertaken was to increase the solubility either by complexation with cyclodextrins or by the formation of eutectic mixtures or cocrystals.

Chapter 4. The active principles from the diazepines class and cyclodextrins systems.

For the considered diazepines, the possible formation of complexes with cyclodextrins, whose solubility may be increased, as reported in the literature, was the end goal. The formation of inclusion complexes is easily highlighted by the disappearance of the melting peak of the pure active substances. In the case of the studied systems, inclusion complexes were not highlighted, as can be seen from figures 8, 9, 10 and 11.

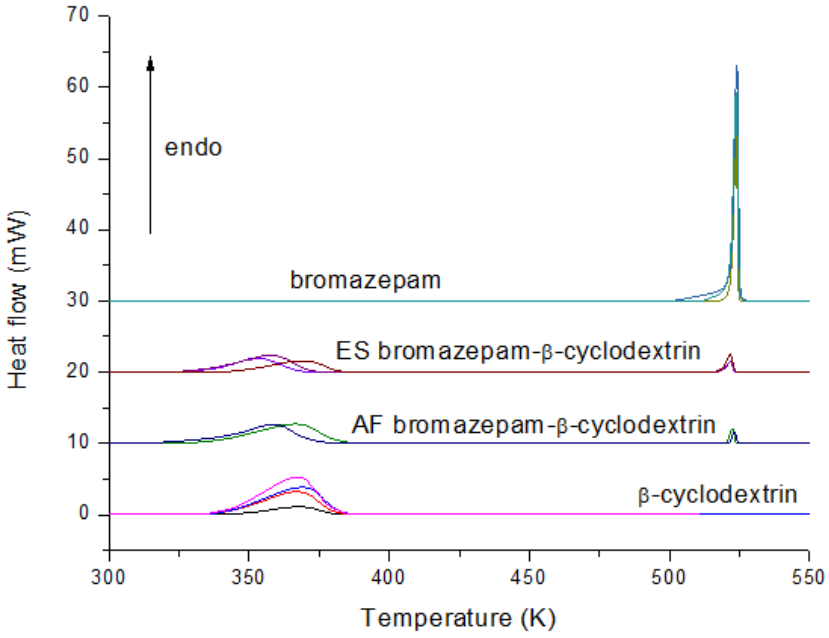

Figure 8. DSC curves of β-cyclodextrin, bromazepam and their mixtures (molar ratio 1:1) prepared by physical mixing (AF) or solvent evaporation method (ES) using water/ethanol as solvent.

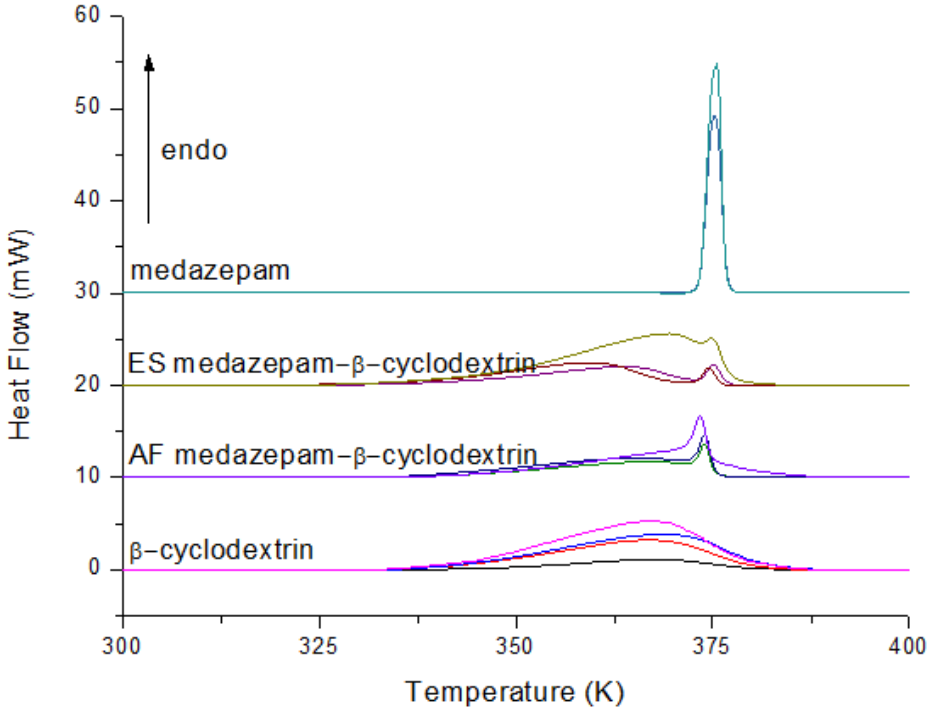

Figure 9. DSC curves of β-cyclodextrin, medazepam and their mixtures (molar ratio 1:1) prepared by physical mixing (AF) or solvent evaporation method (ES) using water/ethanol as solvent.

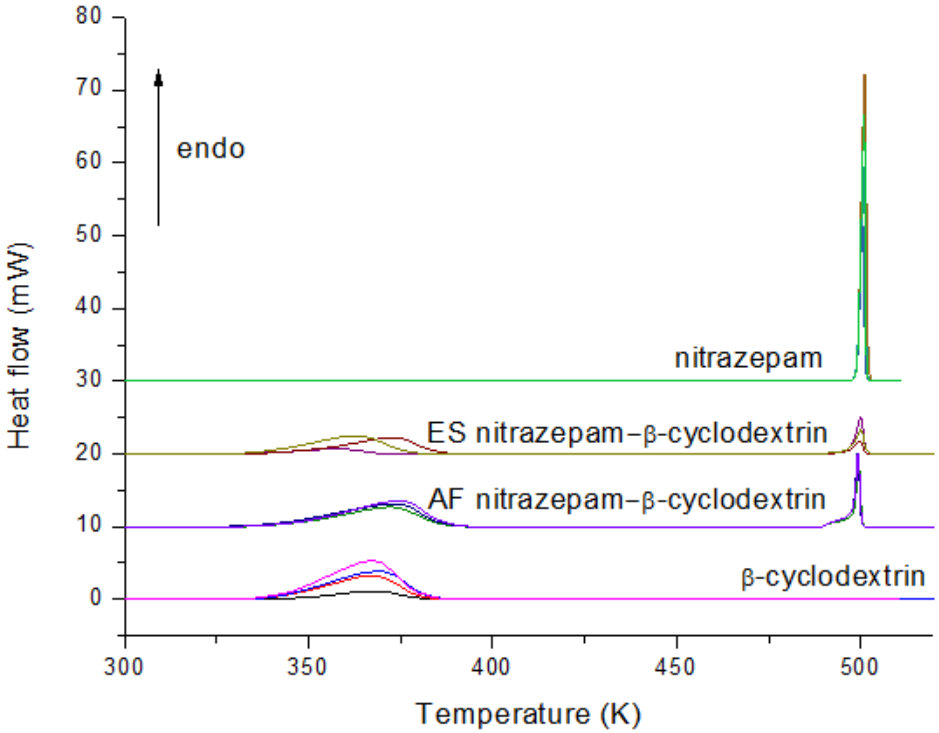

Figure 10. DSC curves of β-cyclodextrin, nitrazepam and their mixtures (molar ratio 1:1) prepared by physical mixing (AF) or by the solvent evaporation method (ES) using water/ethanol as solvent.

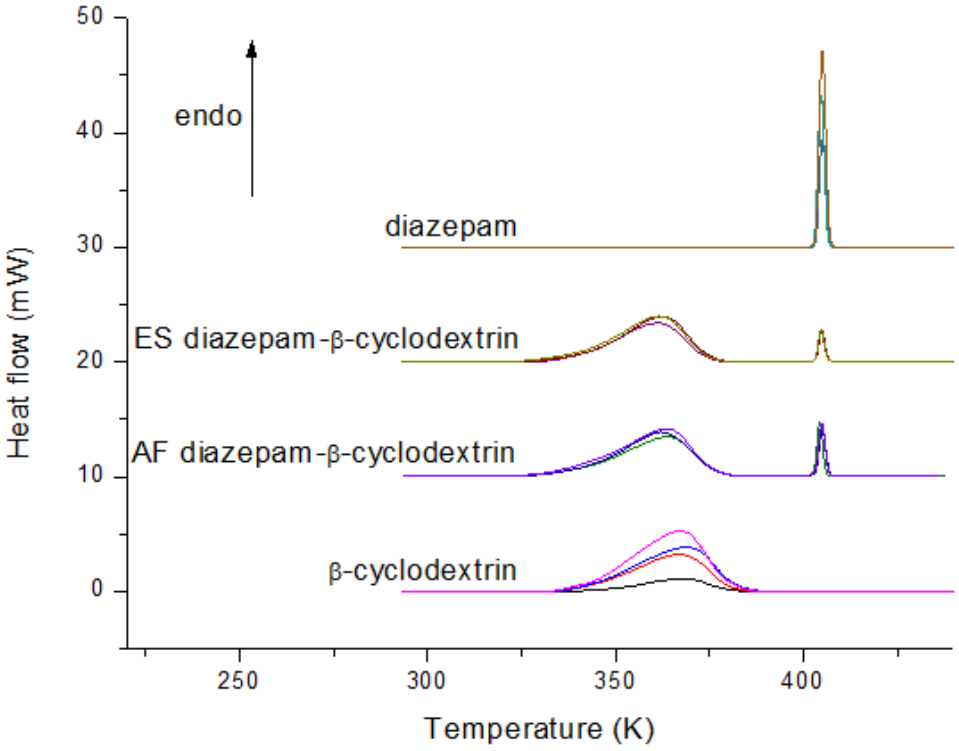

Figure 11. DSC curves of β-cyclodextrin, diazepam and their mixtures (molar ratio 1:1) prepared by physical mixing (AF) or by solvent evaporation method (ES) using water/ethanol as solvent.

The obtained results reoriented the study of increasing solubility through the formation of eutectic/cocrystal mixtures.

Chapter 5. The bromazepam – citric acid system

The results obtained for mixtures by direct and complementary methods are presented in comparison with those of single compounds.

The first eutectic system studied was the bromazepam-citric acid system. The diagrams of differential scanning calorimetry for pure compounds and for binary mixtures made over a wide range of compositions highlight the formation of the eutectic: the first endothermic peak at 390 K can be observed in all mixtures (figure 13). It invariably occurs at a lower melting temperature than that of the individual components, followed by melting of the excess component when the system is not at the eutectic point. The eutectic point occurs at the $x_{bromazepam}$ molar composition of approx. 0.7 when there is virtually no endothermic peak corresponding to the excess component.

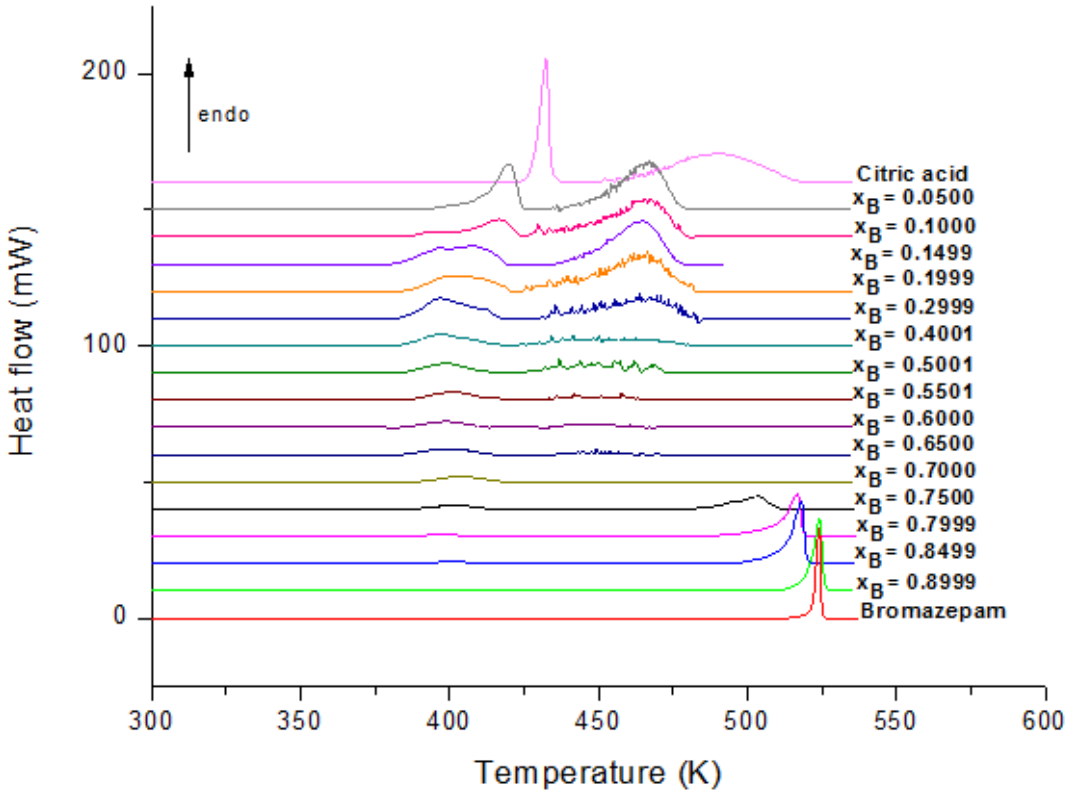

Figure 13. DSC curves of citric acid, bromazepam and their mixtures with the specified compositions.

The experimental phase diagram obtained from DSC measurements is represented by triangles and squares, and the ideal phase diagram obtained with the Schröder - van Laar equation is represented by dots in figure 14.

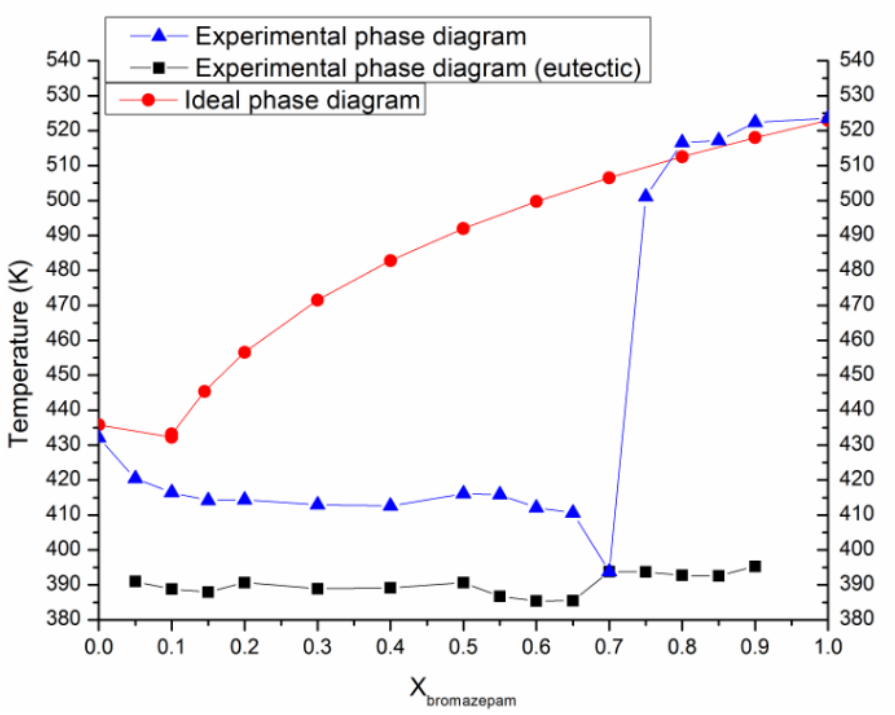

Figure 14. Phase diagram of the bromazepam - citric acid binary mixture.

The experimental data in figure 14 fits the ideal curve only at the extreme of the phase diagram where the mole fraction of bromazepam is greater than 0.8. In the rest of the curve, a deviation from the ideal behavior can be observed, which highlights interactions between the two components, interactions that are expected to lead to an increase in solubility over the entire region of compositions delimited by these two curves.

The nature and type of interactions can be defined with the help of thermodynamic excess functions as a deviation from the ideal system. The values of the excess thermodynamic functions and the activity coefficients are shown in figure 15.

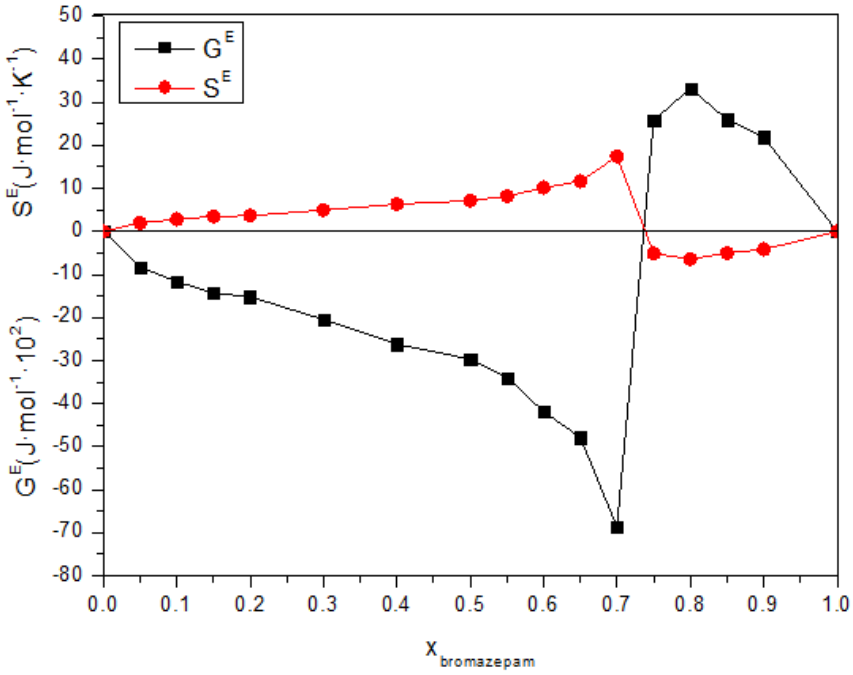

Figure 15. Variation of excess thermodynamic functions with bromazepam mole fraction.

The type of interactions which occurs between the components is given by the value and sign of the excess Gibbs free energy. Thus, the Gibbs free energy of excess has a negative value until it reaches the composition $x_{bromazepam}$ = 0.74, which indicates the presence of weak interactions between molecules of the same type and strong interactions between different molecules. For $x_{bromazepam}$ > 0.74 the excess Gibbs free energy has a positive value which suggests the existence of weak interactions between the components forming the eutectic melt and strong associations between molecules of the same type.

Data obtained by differential scanning calorimetry are confirmed and supported by spectral methods and solubility tests. The FTIR spectra of the mixture highlight both citric acid and bromazepam peaks, with small deviations in the wave number, which indicates the presence

of intermolecular interactions between the two compounds, mainly hydrogen bond formation between the (O-H) of to citric acid and (C=N) from bromazepam.

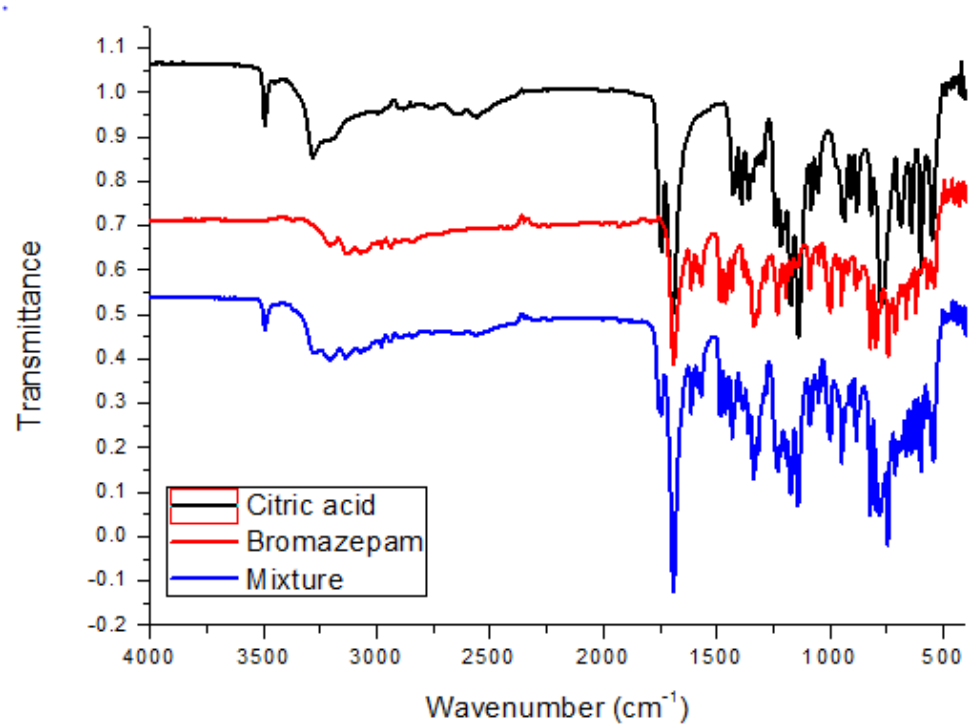

Figure 16. FTIR spectra of citric acid, bromazepam and their eutectic mixture.

Experimental X-ray diffraction data (figure 19-20) confirms the coexistence of the two components of the crystalline phases in bromazepam: anhydrous citric acid mixtures, excluding the formation of other crystalline phases in detectable amounts.

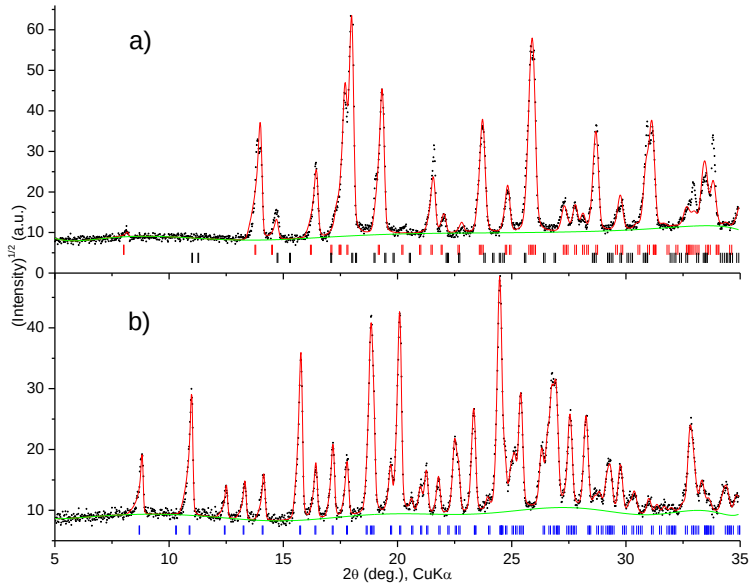

Figure 19: Experimental (black dots) and calculated (red curve) powder X-ray diffractograms for: a) citric acid and b) bromazepam. The short vertical lines mark the positions of indexed

Bragg reflections in monoclinic P21/a (anhydrous citric acid, red), orthorhombic P212121 (monohydrate citric acid, black), and monoclinic P21/c (bromazepam, blue) symmetries.

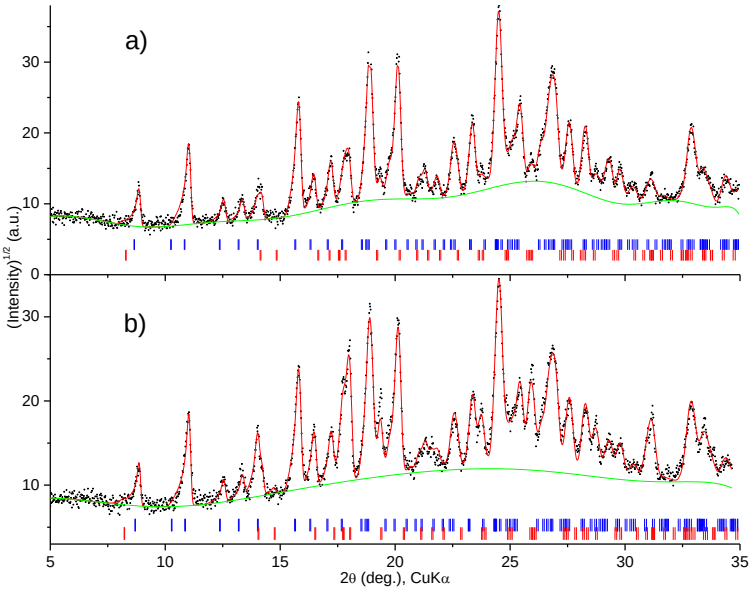

Figure 20: Experimental and calculated powder X-ray diffractograms for bromazepam:anhydrous citric acid mixtures: a) 0.7999: 0.1999 (mol/mol) and b) 0.5501: 0.4502 (mol/mol). Short vertical lines mark the positions of the Bragg reflections for citric acid (red) and bromazepam (blue).

Dissolution tests on bromazepam and the eutectic mixture demonstrated that this system can be applied in practice. Dissolution tests were performed in 0.1 M HCl to simulate gastric fluid. From the dissolution profile of bromazepam (figure 18), it can be seen that the active principle dissolves slowly, the dissolution being complete after 30 minutes, while bromazepam from the eutectic mixture with citric acid dissolved quickly within 5 minutes.

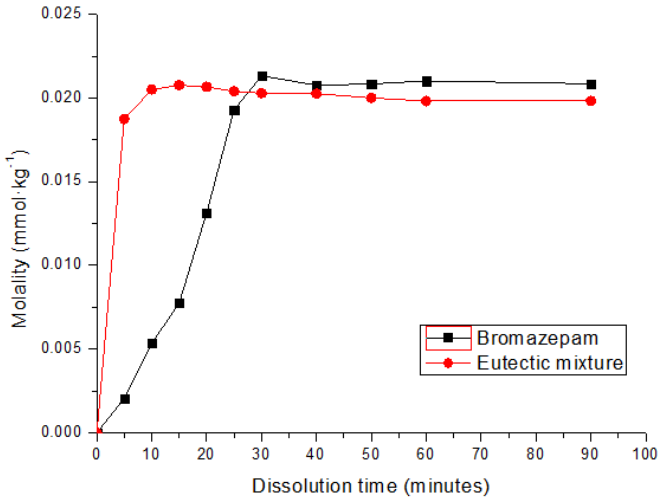

Figure 18: Dissolution profiles of bromazepam and its eutectic mixture with citric acid.

Chapter 6. The nitrazepam – citric acid system

Another system studied was the nitrazepam-citric acid system. The DSC curves for the pure compounds and for the binary mixtures highlight the formation of the eutectic: the first endothermic peak at 396 K can be observed in all mixtures, followed by the melting of the excess component (figure 22).

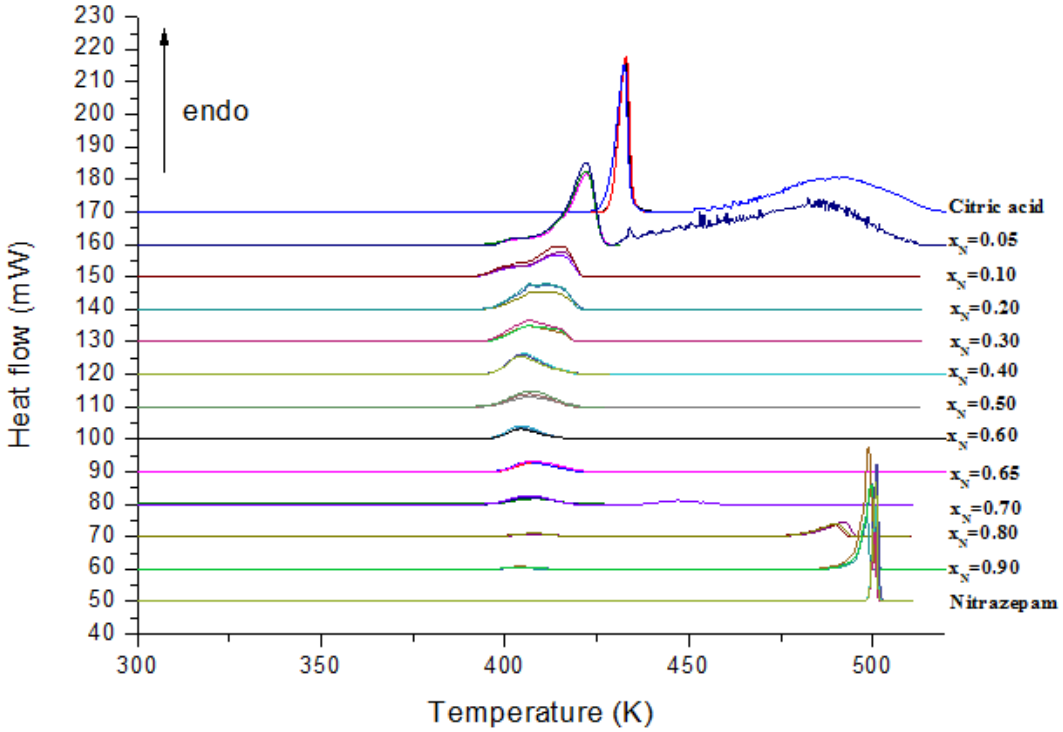

Figure 22. DSC curves for citric acid, nitrazepam and their binary mixtures with the indicated compositions.

For the nitrazepam mole fractions of 0.0500, 0.1000, 0.2015 and 0.3002 a peak deconvolution was required. This was done using the Peak Analyzer function in the Origin software also using Gaussian fitting. The obtained results are shown in figure 23.

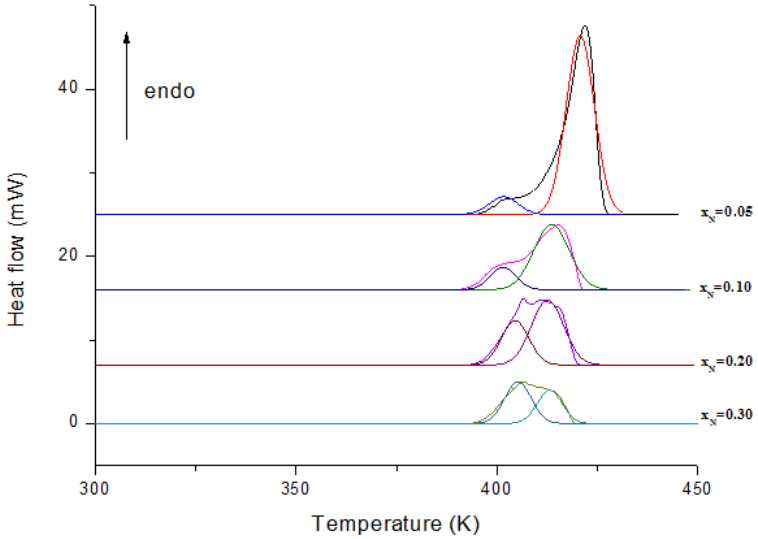

Figure 23: Deconvolution of peaks for binary mixtures with nitrazepam mole fraction 0.0500, 0.1000, 0.2015 and 0.3002.

From this deconvolution, the enthalpy and melting temperature values corresponding to the eutectic and the excess component - citric acid peaks were obtained.

The values of enthalpy and melting temperatures obtained were further used for the construction of Tamman's triangle (figure 24) and the phase diagram (figure 25).

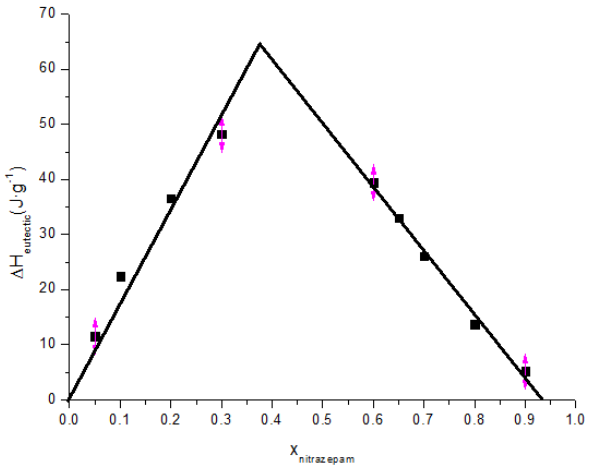

Figure 24. Tamman's triangle obtained for the nitrazepam-citric acid binary mixture.

For a simple eutectic system, the Tamman diagram is represented by a triangle. As seen in figure 24, the enthalpy value of the eutectic peak increases linearly up to the eutectic point ($x_{nitrazepam}$ = 0.3746) after which it decreases with a linear dependence. The points of intersection of the composition axis with Tamman's triangle delineate the compositions at which solid solutions can occur. The results presented in figure 24 shows

that solid solutions must form at the extremities of the phase diagram above $x_{nitrazepam}$ = 0.9332.

In conclusion, it can be said that the binary system nitrazepam - citric acid presents a eutectic point at the molar fraction of nitrazepam $x_{nitrazepam}$= 0.4.

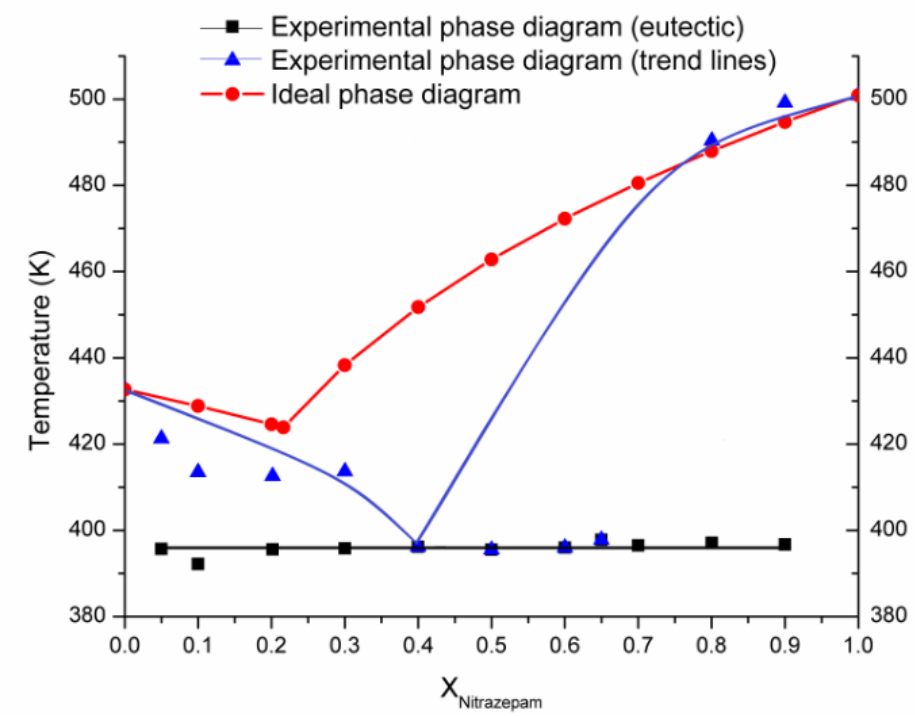

Figure 25. Phase diagram of the binary nitrazepam – citric acid mixtures.

In figure 25, the experimental phase diagram, obtained from DSC data, is symbolized by triangles and squares and the ideal one is symbolized by points and is obtained from the Schröder - van Laar equation.

As seen in figure 25, the experimental data follows the ideal curve only at the extreme of the phase diagram at the nitrazepam mole fraction of 0.8–1.0. Otherwise, a deviation from the ideal behavior is observed. This highlights interactions between the two compounds, interactions that can cause an increase in solubility over the entire region of the compositions delimited by these two curves.

Determining the type of interactions that occur between components is done using the excess Gibbs free energy criterion. It is observed that the excess Gibbs free energy has a negative value until it reaches the molar composition of nitrazepam of 0.7, which shows that there are weak interactions between molecules of the same kind and stronger ones between different molecules. For mole fractions of nitrazepam greater than 0.7, the Gibbs free energy of excess has a positive value, which suggests the existence of weak

interactions between the components that form the eutectic melt and strong associations between the same molecules.

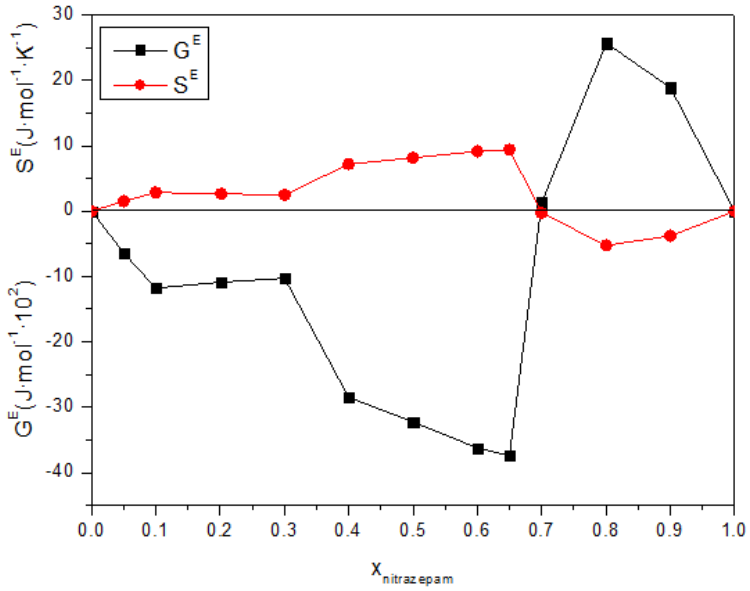

Figure 26. Variation of excess thermodynamic functions with nitrazepam composition.

The FTIR experiments show that the eutectic mixture has a spectrum containing both citric acid and nitrazepam peaks, with small deviations in wavenumber. These deviations show that there are intermolecular interactions between the two compounds, mainly hydrogen bonds between the (O-H) of citric acid and the (C=N) of nitrazepam.

Experimental XRD diffractograms showed the coexistence of two crystalline phases in the nitrazepam - anhydrous citric acid eutectic mixture, with no evidence for the formation of detectable amounts of other crystalline phases.

The eutectic mixture was further chosen to evaluate the solubility of nitrazepam in aqueous medium.

The results of the solubility experiment are shown in Table 6.

Table 6. Solubility of nitrazepam in two media (deionized water and simulated gastric fluid).

Medium used to determine solubility	Solubility (μg·mL^{-1})	
	Nitrazepam	Eutectic
Deionized water	37.05	49.07
Simulated gastric fluid	104.1	102.6

In the simulated gastric fluid environment, the solubility of nitrazepam by itself and in the eutectic was studied and obtained: 104.1 $\mu g \cdot mL^{-1}$ for pure nitrazepam and 102.6 $\mu g \cdot mL^{-1}$ for the eutectic, values considered to be approximately identical. At neutral pH - the amount of nitrazepam in the samples was: 37.05 $\mu g \cdot mL^{-1}$ for the single nitrazepam and 49.07 $\mu g \cdot mL^{-1}$ for the eutectic.

Although a solubility increase of nitrazepam in the eutectic is expected, the studies carried out highlight that this is due to the acidic character of citric acid, therefore the solubility depends on the pH of the environment (the solubility of the eutectic increases by 32% in a neutral environment, deionized water).

Chapter 7. The medazepam – citric acid system

Another system studied was the medazepam-citric acid system.

The DSC curves of the pure compounds and the binary mixtures are shown in figure 30 and 31. For the medazepam mole fractions of 0.9003 and 0.9519, a deconvolution of the peaks was required because the two DSC peaks are not well separated. From figure 30 it can be seen that the formation of the eutectic always occurs at a lower temperature than that of the single components, followed by the melting of the excess component.

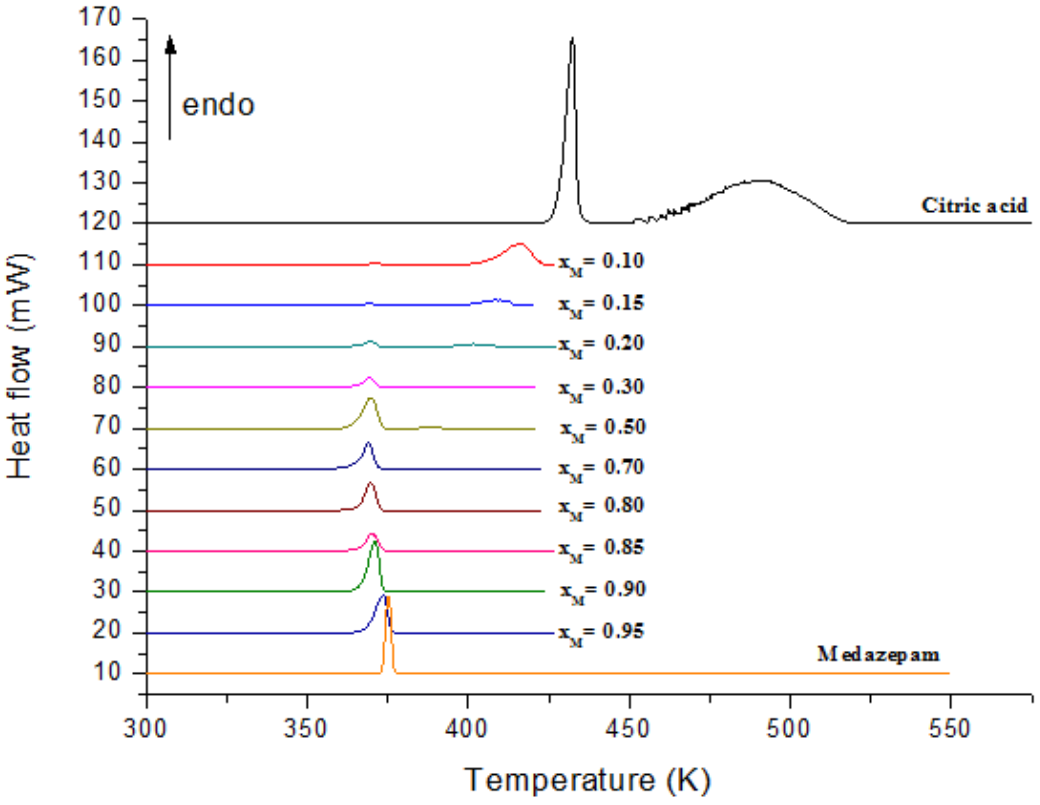

Figure 30. DSC curves for medazepam, citric acid and their binary mixtures.

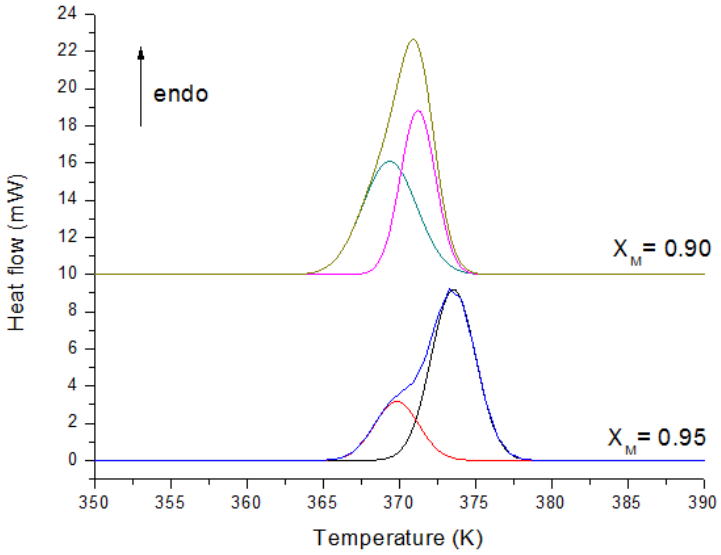

Figure 31: Peak deconvolution for binary mixtures with medazepam mole fraction 0.9003 and 0.9519.

The eutectic composition can be accurately determined only from Tamman's triangle. This is a plot of eutectic peak enthalpy versus mole fraction (figure 32). To build this graph, in the case of the molar fraction of 0.90 and 0.95, the data obtained from the deconvolution of the peaks were used. A eutectic system is represented by a triangle in the Tamman diagram. As can be seen in figure 32, the eutectic enthalpy value increases linearly until it reaches the eutectic point ($x_{medazepam}$ = 0.8565), after which it decreases linearly. The points of intersection of the mole fraction axis with Tamman's triangle delineate the mole fractions at which solid solutions can occur. The results presented in figure 32 shows that solid solutions must form at the extremities of the phase diagram above $x_{medazepam}$ = 0.9865.

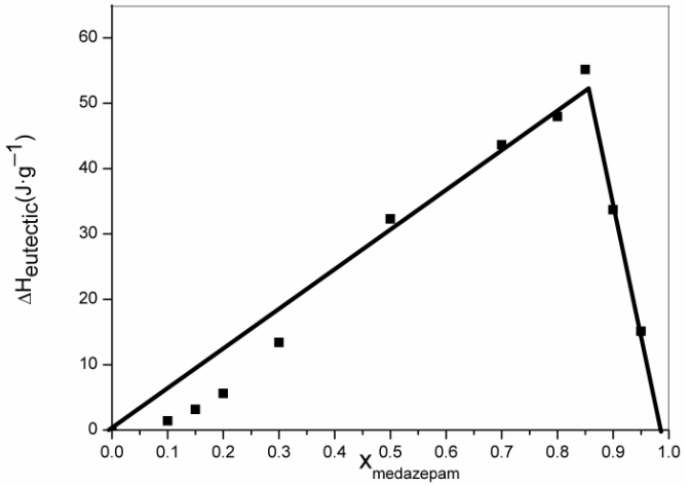

Figure 32. Tamman's triangle.

Figure 33 shows the phase diagram of the considered binary system. A simple eutectic point constituted by the first endothermic peak, placed approximately at 370 K is present for all compositions. In conclusion, it can be said that the binary system medazepam - citric acid presents a eutectic at the molar fraction of medazepam $x_{medazepam}$= 0.85.
In the figure, the experimental phase diagram obtained from DSC data is symbolized by triangles and squares. The ideal diagram, symbolized by dots, is obtained from the Schröder - van Laar equation.

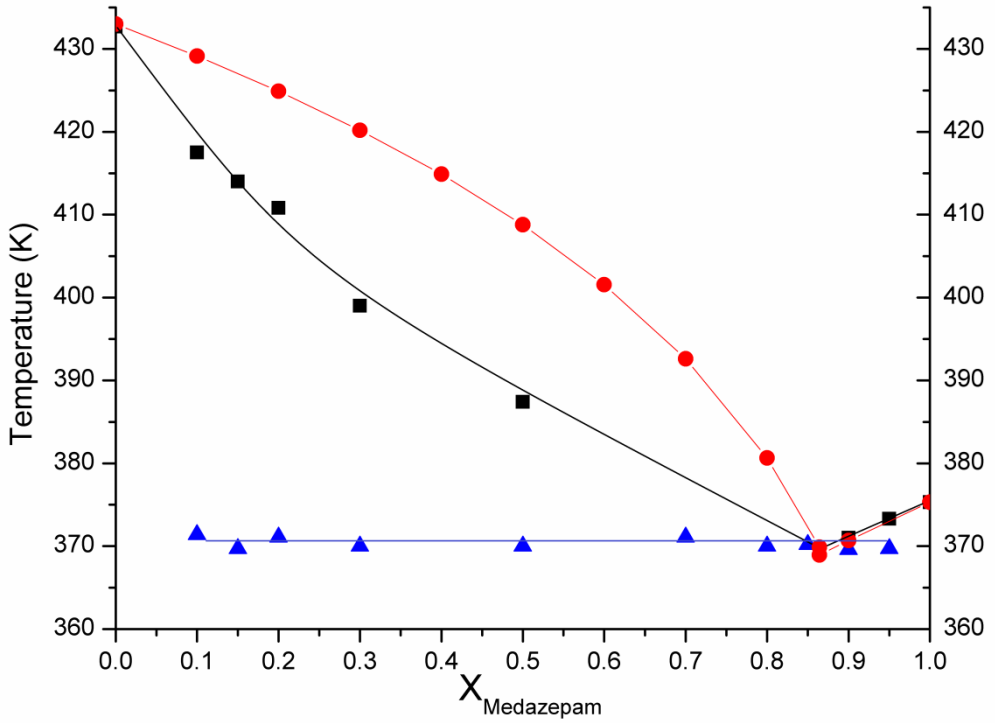

Figure 33. Phase diagram of the medazepam-citric acid system.

Figure 33 shows that the experimental data fits on the ideal curve only in the range of medazepam molar fractions of 0.85-1.0, otherwise it shows deviation from the ideal behavior. It can be concluded that there are interactions between the two components over the entire region of the mole fractions delimited by these two curves.
The nature and type of interactions of a binary system can be defined with thermodynamic excess functions (S^E, G^E and μ^E) as a deviation from ideality.

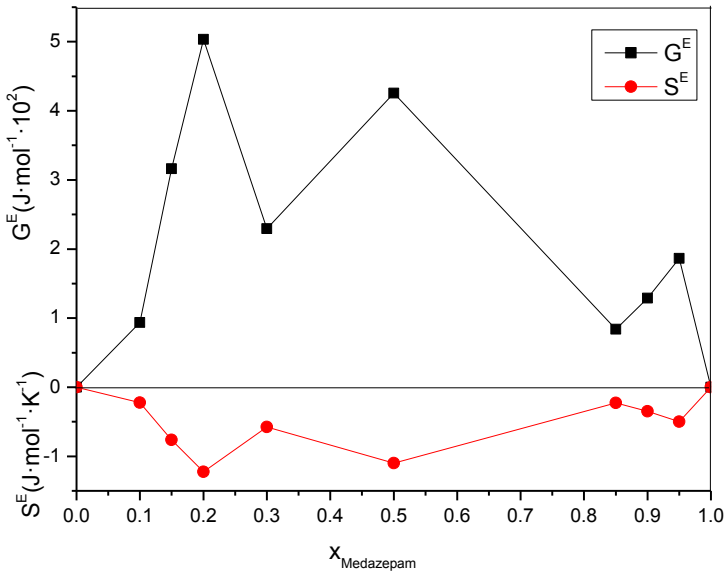

Figure 34. Variation of thermodynamic excess functions with medazepam mole fraction.

As can be seen in figure 34, the Gibbs free energy values have a maximum for the medazepam mole fraction of 0.20 and a minimum for the medazepam mole fraction of 0.85. Excess entropy follows the same increase/decrease patterns as Gibbs free energy, but in mirror form.

The types of interactions that occur between the components are determined by the excess Gibbs free energy. In figure 34, over the entire range of mole fractions of medazepam, the excess Gibbs free energy has a positive value, which suggests the existence of weak interactions between different components and strong associations between molecules of the same kind.

The FTIR spectrum of the eutectic mixture contains both citric acid and medazepam peaks with small deviations.

These deviations highlight intermolecular interactions between the two compounds, mainly hydrogen bonds between (O-H) of citric acid and (C-Cl) of medazepam.

Solubility tests showed that the solubility of medazepam in deionized water is 0.73 µg/mL. For medazepam in the eutectic mixture, the solubility was 28.61 µg/mL indicating an approximately 40-fold increase.

To see which parameter influences solubility the most (acidic character of the coformer / eutectic formation), a solubility test was performed for medazepam in 0.1 M

HCl. When the experiment was performed using this medium, the entire amount of medazepam was solubilized, crossing the threshold from practically insoluble to soluble. Considering that the human stomach has a low pH environment, orally administered drugs do not require improvements in solubility aspects. However, the results can easily be applied to parenteral, topical or suppository pharmaceutical forms.

Chapter 8. The meloxicam – tartaric acid system

The last system studied in the thesis was the system consisting of meloxicam and tartaric acid. Preliminary tests with citric acid and meloxicam showed no eutectic or cocrystal formation. In this context, tartaric acid, often used in the pharmaceutical industry, which belongs to the same class of compounds as citric acid, was used as an excipient.

The DSC curves obtained for the cocrystallization product from solvent-assisted mechanosynthesis are shown in figure 37. The results show two endothermic peaks at 447.7 K and 527.7 K for pure tartaric acid and one endothermic peak at 538.2 K for pure meloxicam. Interestingly, the cocrystal product also exhibits two endothermic peaks at 442.0 and 552.3 K, separated by a broad exothermic peak. Although this can be interpreted as a transition between enantiotropic polymorphic forms of the cocrystal, such behavior is relatively unusual, which is why thermogravimetric analysis tests were performed (figure 38). They showed that the exothermic peak and the second endothermic peak signal degradation processes.

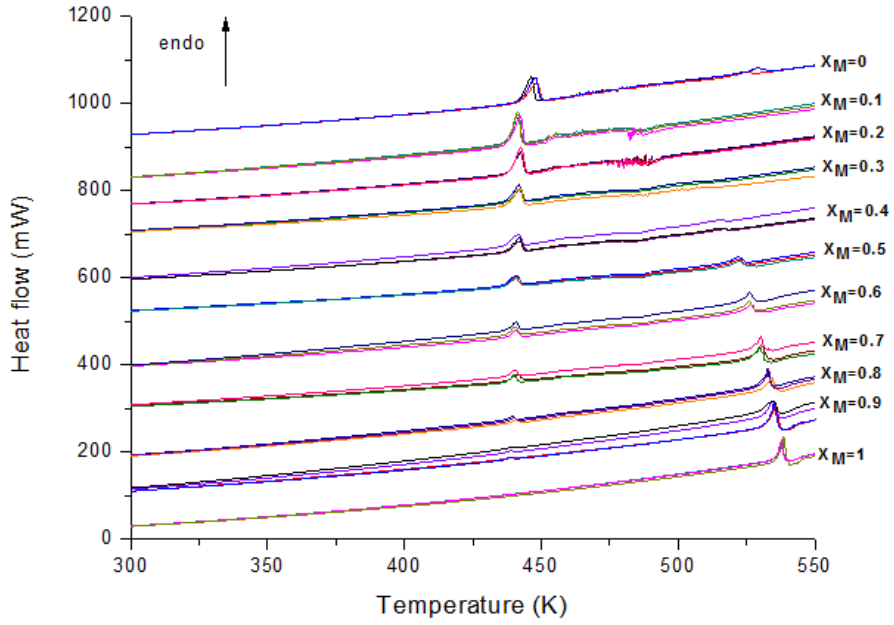

Figure 37. DSC curves for tartaric acid, meloxicam and their binary mixtures.

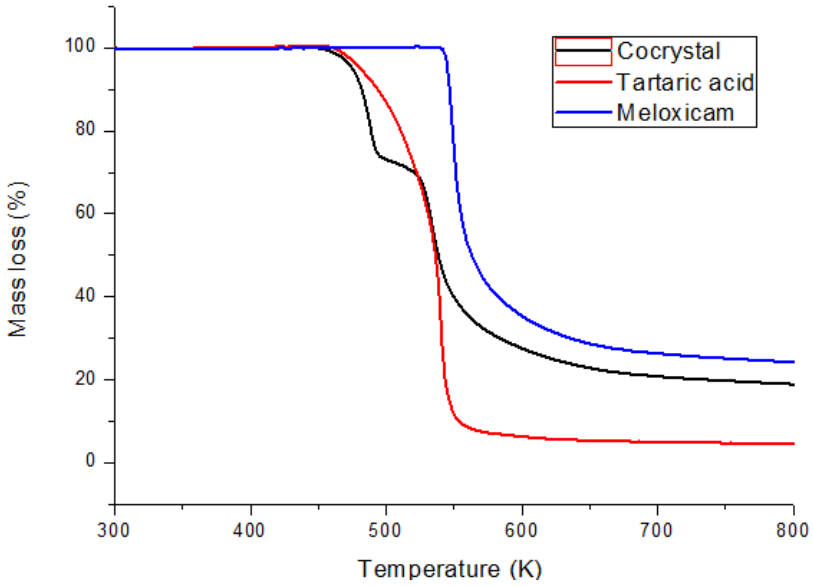

Figure 38. Thermogravimetric analysis curves for tartaric acid, meloxicam and their binary mixtures.

The FTIR study for tartaric acid, meloxicam and their cocrystal showed variations in the spectrum of the cocrystal compared to the pure compounds which highlight intermolecular interactions between the two compounds, mainly hydrogen bonds between (-NH) of meloxicam and (-C=O) from tartaric acid.

The XRD patterns of tartaric acid, meloxicam and their co-crystal show the characteristic diffraction lines of meloxicam at 11.2°, 13.0°, 14.8°, 17.8°, 18.5°, 19.2° and 25.8° and those of tartaric acid at 16.8°, 20.2 °, 20.6°, 28.9°, 29.6°, 31.8°, 31.9°, 33.1° and 39.2°. The XRD diffractograms of the cocrystal show differences in diffraction peaks with its own unique diffraction peaks at 31.6° and 32.0°, and some peaks characteristic of tartaric acid disappear (16.8°, 28.9°, 31.8°, 31.9°, 33.1° and 39.2°) . Therefore, the disappearance and shift of the peaks further confirmed the formation of meloxicam-tartaric acid cocrystal.

Solubility tests for meloxicam and its tartaric acid cocrystal in deionized water show that the solubility of meloxicam was 8.62 µg/mL and for meloxicam in the cocrystal its solubility was 0.13 µg/mL in deionized water indicating a decrease in meloxicam solubility in the cocrystal. This can be explained due to its low solubility in acidic and neutral conditions.

However, a new direction of research is opened for meloxicam-compound binary mixtures with a basic character. Preliminary tests have shown an improvement in solubility in basic media.

General conclusions

The aim of the work was to improve the solubility of the active principles through the formation of eutectics or cocrystals. From all the methods in the literature, thermal analysis was used as the main technique to distinguish the type of systems formed and the confirmation was made with complementary methods: X-ray diffraction and Fourier transform infrared spectroscopy.

Three substances from the benzodiazepine class were used as active principles, namely bromazepam, nitrazepam and medazepam, with sedative, calming and muscle-relaxing effects that must be quickly absorbed by the body. In addition to these three active principles, meloxicam, a nonsteroidal anti-inflammatory drug used to relieve mild to moderate pain that needs rapid absorption into the body, was also studied.

An attempt was first made to increase the solubility of the active principles by forming inclusion complexes, but DSC tests showed that these complexes do not form.

In order to increase the solubility of the active principles, we then tried to obtain eutectic systems and co-crystals, which, according to literature data, could lead to an increased solubility of the substance of interest.

Thus, the bromazepam-citric acid eutectic system was obtained. DSC tests showed the presence of a eutectic point at $x_{bromazepam}$ = 0.7 and temperature 390 K. FTIR revealed the presence of hydrogen bonds in the eutectic. X-ray diffraction tests show that no other crystalline phases form in the eutectic and dissolution studies demonstrate that the eutectic mixture has a higher solubility.

Another eutectic system prepared was nitrazepam-citric acid where DSC data showed the presence of a eutectic point at $x_{nitrazepam}$=0.4 and temperature 396 K. FTIR tests only show the formation of hydrogen bonds and XRD data showed the presence of two crystalline phases in the mixture eutectic, without the formation of additional crystalline phases. The solubility tests carried out show that it depends on the pH of the environment (the solubility of the eutectic increases by 32% in neutral environment, deionized water).

The medazepam-citric acid eutectic system was also studied. DSC data shows a eutectic point at $x_{medazepam}$=0.85 and temperature 370 K. FTIR data shows no significant changes and thus eutectic formation is confirmed. The solubility tests performed showed that the solubility of medazepam in water was significantly improved in the eutectic mixture. Tests performed in acidic medium reveal that the acidic character of the excipient influences solubility more than

eutectic formation. However, it has been significantly improved and can be used in the pharmaceutical industry for parenteral, topical or suppository forms.

The last binary system studied in the thesis was meloxicam and tartaric acid. DSC data show the presence of a cocrystal at $x_{meloxicam} = 0.5$. FTIR spectra highlight the formation of hydrogen bonds. X-ray diffraction shows the formation of the cocrystal by the disappearance/shifting/appearance of diffraction lines in its spectrum. Solubility tests performed on the cocrystal reveal that it has a lower solubility due to the acidic character of tartaric acid.

References:

18. E. Stoler, J. Warner. Non-Covalent Derivatives: Cocrystals and Eutectics. Molecules 2015, 20, 14833-14848. doi:10.3390/molecules200814833.

28. M. Jagia, R. Daptardar, K. Patel, A. Bansal, S. Patel. Role of Structure, Microenvironmental pH, and Speciation To Understand the Formation and Properties of Febuxostat Eutectics. Mol. Pharmaceutics 2019. doi: 10.1021/acs.molpharmaceut.9b00716.

29. D. Elder, R. Holm, H. Diego. Use of pharmaceutical salts and cocrystals to address the issue of poor solubility. Int. J. Pharm. 2012.https://doi.org/10.1016/j.ijpharm.2012.11.028.

31. G. Bruni, L. Maggi, P. Mustarelli, M. Sakaj, V. Friuli, C. Ferrara, V. Berbenni, A. Girella, C. Milanese, A. Marini. Enhancing the Pharmaceutical Behavior of Nateglinide by Cocrystallization: Physicochemical Assessment of Cocrystal Formation and Informed Use of Differential Scanning Calorimetry for Its Quantitative Characterization. J. Pharm. Sci. 2019, 108, 1529–1539.

38. S. Emami, M. Siahi-Shadbad, M. Barzegar-Jalali, K. Adibkia. Characterizing eutectic mixtures of gliclazide with succinic acid prepared by electrospray deposition and liquid assisted grinding methods. J. Drug. Deliv. Sci. Technol. 2018, 45, 101–109.

39. R. Patel, M. Raval, T. Pethani, N. Sheth. Influence of eutectic mixture as a multi-component system in the improvement of physicomechanical and pharmacokinetic properties of diacerein. Adv. Powder Technol. 2020, 31, 1441–1456.

45. S. Cherukuvada, A. Nangia. Fast dissolving eutectic compositions of two anti-tubercular drugs. CrystEngComm. 2012, 14, 2579.

80. Meltzer, „Termodinamică Chimică”, Ed. Universității din București, București 2007.

82. D. C. Marinescu, E. Pincu, V. Meltzer. Thermal analysis of binary liquid crystals eutectic system cholesteril p-phenoxi phenyl carbamate–cholesteril p-biphenyl carbamate. J. Therm. Anal. Calorim. 2011, 110, 985-990.

84. G.G. Chernick. Phase equlibria in phospholipid water systems. Adv. Colloid Interface Sci. 1995, 61, 65-129.

85. S. Lerdkanchanaporn, D. Dollimore, S. J. Evans. Thermodynamic characterization of binary liquid crystal mixtures. Thermochim. Acta 2001, 8, 367 – 368.

86. U. S. Rai, P. Pandley. Solidification and thermal behaviour of binary organic eutectic and monotectic; succinonitrile–pyrene system. J. Cryst. Growth 2003, 249, 301-308.

88. N. Singh, N. B. Singh, U. S. Rai, O. P. Singh. Structure of Eutectic Melts; Binding Organic Systems. Thermochim. Acta 1985, 95(1), 291-293.

89. B.L. Sharma, R. Kant, R. Sharma and S. Tandon, Deviations of binary organic eutectic melt systems. Mater. Chem. Phys. 2003, 82(1), 216-224.

92. U. S. Rai, R. N. Rai. Chemistry and characterization of binary organic eutectics and molecular complexes. The urea-m-nitrobenzoic acid system. Mater. Lett. 1998, 34, 67 – 75.

97. A. Chauhan, P. Chauhan. Powder XRD Technique and its Applications in Science and Technology. J. Anal. Bioanal. Tech. 2014, 5, 212. doi: 10.4172/2155-9872.1000212.

99. B.C. Smith. Fundamentals of Fourier Transform Infrared Spectroscopy, CRC Press, Francis & Taylor Group, Boca Raton, 2011.

100. M. Davis, M. Brewster. Cyclodextrin-Based Pharmaceutics: Past, Present and Future, Nat. Rev. Drug Discov. 2004. doi: 10.1038/nrd1576.

110. P. Thompson, D. E. Cox, J. B. Hastings. Rietveld refinement of Debye-Scherrer synchrotron X-ray data from Al2O3. J. Appl. Cryst. 1987, 20, 79-83

125. D. Marinescu, E. Pincu, I. Stanculescu, V. Meltzer, Thermal and spectral characterization of a binary mixture (acyclovir and fluocinolone acetonide): Eutectic reaction and inclusion complexes with β-cyclodextrin, Thermochim. Acta 2013, 560, 104–111.

131. D. Marinescu, E. Pincu, V. Meltzer. Thermodynamic study of binary system Propafenone Hydrocloride with Metoprolol Tartrate: Solid–liquid equilibrium and compatibility with α-lactose monohydrate and corn starch. Int. J. Pharm. 2013, 448, 366–372.

141. S. Cherukuvada, A. Nangia. Eutectics as improved pharmaceutical materials: Design, properties and characterization. Chem Commun 2014, 50, 906–923.

142. S. Cherukuvada, T. N. G. Row. Comprehending the Formation of Eutectics and Cocrystals in Terms of Design and Their Structural Interrelationships. Cryst Growth Des 2014, 14, 4187–4198.

144. G. Bruni, M. Sakaj, V. Berbenni, L. Maggi, V. Friuli, A. Girella, C. Milanese, A. Marini. Physico-chemical and pharmaceutical characterization of sulindac–proglumide binary system. J Therm Anal Calorim 2018. doi.org/10.1007/s10973-018-7858-7.

153. C. Macasoi, E. Pincu, B. Jurca, V. Meltzer. Increasing the bromazepam solubility by forming eutectic mixture with citric acid. Thermochim. Acta 2021, 702, 178954.

158. B. Saikia, A. Seidel-Morgenstern, H. Lorenz. Multicomponent Materials to Improve Solubility: Eutectics of Drug Aminoglutethimide. Crystals 2022, 12, 40.

164. C. Macasoi, E. Pincu, B. Jurca, C. Romanitan, V. Meltzer. Physico-chemical study of nitrazepam and citric acid eutectic mixture. Thermochim. Acta 2023, 724, 179499.

Published scientific papers:

1. Increasing the bromazepam solubility by forming eutectic mixture with citric acid. Macasoi Cristina, Pincu Elena, Jurca Bogdan, Meltzer Viorica. Thermochimca Acta 2021; 702:178954. https://doi.org/10.1016/j.tca.2021.178954 (FI 3.5);
2. Physico-chemical study of nitrazepam and citric acid eutectic mixture. Macasoi Cristina, Pincu Elena, Jurca Bogdan, Romanitan Cosmin, Meltzer Viorica. Thermochimca Acta 2023; 724:179499. https://doi.org/10.1016/j.tca.2023.179499 (FI 3.5);
3. Thermal and spectral characterization of binary mixture medazepam and citric acid: eutectic reaction and solubility studies. Macasoi Cristina, Meltzer Viorica, Pincu Elena. Thermo 2023; 3(3): 483-493. https://doi.org/10.3390/thermo3030029.